Simulation of Diffusion Anisotropy in DTI for Virtual Cardiac Fiber Structure

Lihui Wang[1,2], Yue-Min Zhu[2], Hongying Li[2],
Wanyu Liu[1,2], and Isabelle E. Magnin[2]

[1] Harbin Institute of Technology, 150001, Harbin, China
[2] CREATIS, CNRS UMR5220, Inserm U1044, INSA Lyon, University of Lyon1,
University of Lyon. 69100 Villeurbanne, France
{lihui.wang,yuemin.zhu,hongying.li,
isabelle.magnin}@creatis.insa-lyon.fr
wanyu.liu@hit.edu.cn

Abstract. Diffusion anisotropy is the most fundamental and important parameter in the description of cardiac fibers using diffusion tensor magnetic resonance imaging (DTI), by reflecting the microstructure variation of the fiber. It is, however still not clear how the diffusion anisotropy is influenced by different contiguous structures (collagen, cardiac myocyte, etc.). In this paper, a virtual cardiac fiber structure is modeled, and diffusion weighted imaging (DWI) and DTI are simulated by the Monte Carlo method at various scales. The influences of the water content ratio in the cytoplasm and the extracellular space and the membrane permeability upon diffusion anisotropy are investigated. The simulation results show that the diffusion anisotropy increases with the increase of the ratio of water content between the intracellular cytoplasm and the extracellular medium. We show also that the anisotropy decreases with the increase of myocyte membrane permeability.

Keywords: DTI, cardiac myocyte, diffusion anisotropy, myocardial fiber, Monte Carlo simulation.

1 Introduction

The myocardial fiber structure plays an important role in determining the mechanical and electrical properties of the ventricles of the human heart. It is very useful for analyzing the normal and pathologic states of the heart. Up to now, most research on myocardial fiber structure focuses on fiber orientation, which can be provided by diffusion magnetic resonance imaging (DMRI). DMRI measures the displacement of water molecules subject to Brownian motion within the tissues. Since the mobility of the molecules is conditioned by the microstructure of the tissue, especially the direction, we can infer the structural orientation information of the later from the anisotropy of the molecular displacements.

A number of approaches for analyzing the DMRI have been proposed, and the most popular ones are diffusion tensor magnetic resonance imaging (DTI) [1, 2], high angular resolution diffusion imaging (HARDI) [3], q-space imaging (QSI) [4] and

D.N. Metaxas and L. Axel (Eds.): FIMH 2011, LNCS 6666, pp. 95–104, 2011.

q-ball imaging (QBI) [5]. These methods provide more and more precise knowledge about the orientation distribution of fibers. However, for typical DMRI, an image voxel is of the order of about 10 mm^3. For cardiac applications, it means that such voxel contains thousands of cardiac myocytes and other extracellular tissues. In this condition, it would be difficult to know exactly whether the diffusion anisotropy measured by the above imaging modalities arises from the intra myocyte compartment or the extracellular compartment or their combination [6,7]. Meanwhile, the diffusion of water molecules in each compartment (e.g., collagen, intercalated disk, membrane, and cytoplasm) is affected by the local viscosity, component, geometry and membrane permeability, etc. As a result, using DMRI techniques, it is impossible to analyze the influence of these factors on diffusion anisotropy, because of the so small size of myocytes, whose length ranges from 50~100μm, and diameter from 10~25μm [8].

In order to overcome the technical limitations of these imaging techniques, several modelling and simulation methods have been developed. In [9], the Brownian motion of molecules by the Monte Carlo (MC) was simulated in a restricted space to obtain the diffusion signal. The authors of [10] introduced the concept of spin phase memory loss during the MC simulation and applied it to describe the diffusion-induced signal attenuation. In [11] the diffusion anisotropy was simulated with the digital fiber phantom. The authors of [12] compared the experimental diffusion signal and the simulated signal for a cylinder fiber. In the present work, we propose to model virtual cardiac fiber structures (VCFS) and simulate the diffusion behavior of water molecules in this VCFS. We use the quantum spin theory to compute virtual diffusion magnetic resonance (MR) images and analyze the contribution of various structure parameters (such as water content in extracellular space and intracellular cytoplasm) and the membrane permeability to the diffusion anisotropy. The rest of this paper is organized as follows. The simulation method is presented in Section 2, the obtained results and discussion in Section 3, and the conclusion in Section 4.

2 Method

2.1 VCFS Model

In order to mimic the realistic structure of a myocyte as well as that of a myocardial fiber, and find an easy way to describe some of known variations in the tissue structure, such as the shape and the location of the myocyte, and their small shape variation during the beat of the heart, we model the VCFS as a three-dimensional matrix of realistically shaped myocytes organized into fibers. They are connected with intercalated disks and plunged in within an extracellular medium. In order to reduce computation consuming resources, the spatial resolution of the model was selected as 5 μm. The model consists of the mixture of two regions, the intracellular cytoplasm and the extracellular space. Each myocyte in the model has a size of about 15×25×90 μm^3 and all the myocytes share the same direction along the long axis but they are arranged differently in space, which means from a macroscopic viewpoint, that the anisotropy is uniform, but from a microscopic view, it is not.

2.2 Diffusion MRI Simulation Theory

The diffusion process can be seen as a sequence of small random walks of water molecules. If the walk of molecules obeys the stochastic properties of a Brownian particle, the random 3D walking displacement $\Delta\vec{r}_i$ of a molecule i during time interval δt between two random walks is then given by [12]:

$$\Delta\vec{r}_i = \sqrt{6D_0\delta t} \quad . \tag{1}$$

where D_0 is the diffusion coefficient of water molecules.

According to the basic theory of DMRI [13], the phase shift induced by this displacement is

$$\Delta\phi_i = 2\pi\vec{q}\cdot\Delta\vec{r}_i \quad . \tag{2}$$

where $\vec{q}$ is related to the diffusion gradient $\vec{G}(t)$, $q = \frac{\gamma}{2\pi}\int\vec{G}(t)dt$ and γ is the gyromagnetic ratio.

Thus, the diffusion signal can be numerically approximated by

$$E(\Delta\phi) = \frac{1}{n}\sum_{i=1}^{n}\cos(\Delta\phi_i)\ ; \qquad \Delta\phi_i \in P(\Delta\phi) \quad . \tag{3}$$

where n designates the number of molecules involved and i the index of the molecules. The phase $\Delta\phi_i$ should conform to the distribution $P(\Delta\phi)$. By combining equations (2) and (3), the diffusion signal can be further written as

$$E(\phi) = \frac{1}{n}\sum_{i=1}^{n}\cos(2\pi\vec{q}\cdot\Delta\vec{r}_i)\ ; \qquad \Delta\vec{r}_i \in P(\Delta\vec{r}) \quad . \tag{4}$$

If the diffusion gradient is a constant, according to equation (2), the distribution of $P(\Delta\vec{r})$ will be the same as that of $P(\Delta\phi)$. In our research, this distribution is simulated by a Monte Carlo method. Designating the diffusion time as Δ, then the number of random walk steps m for one molecule is

$$m = \frac{\Delta}{\delta t} \quad . \tag{5}$$

If the displacement for the i^{th} molecule induced by the j^{th} walk step is $\Delta\vec{r}_{ij}$, the corresponding phase shift is

$$\phi_{ij} = 2\pi\vec{q}\cdot\Delta\vec{r}_{ij} \quad . \tag{6}$$

At the end of the diffusion, the total phase shift for the i^{th} molecule is

$$\phi_i = \sum_{j=1}^{m}\phi_{ij} = \sum_{j=1}^{m}2\pi\vec{q}\cdot\Delta\vec{r}_{ij} \quad . \tag{7}$$

According to equation (4), we then obtain the diffusion signal

$$E(\phi) = \frac{1}{n}\sum_{i=1}^{n}\cos(\phi_i) = \frac{1}{n}\sum_{i=1}^{n}\cos(\sum_{j=1}^{m} 2\pi \bar{q}\cdot\Delta\bar{r}_{ij}) \quad . \tag{8}$$

Due to the complex structure of the cardiac fibers, the diffusion of water molecules in the VCFS model is not free. Therefore, the interaction between the molecules and the membrane of the myocyte should be considered in the simulation. In this work, such interaction is modeled by elastic collision and reflection, which means that, after the collision with the membrane, the molecule does not lose energy and will be reflected by the membrane in an arbitrary direction.

Based on the above hypothesis, we add diffusion gradients along different directions to get the diffusion weighted images of the VCFS model. In order to analyze the influence of different parameters upon the diffusion anisotropy, we calculated the diffusion tensor [14, 15] and fractional anisotropy (FA). In the present work, the number of gradient directions was selected as 30, which were obtained from the Siemens MRI machine. Let λ_1 , λ_2 and λ_3 represent respectively the three eigenvalues of the diffusion tensor. The FA is then given by [14, 15]

$$\mathrm{FA} = \sqrt{\frac{1}{2}}\frac{\sqrt{(\lambda_1-\lambda_2)^2+(\lambda_1-\lambda_3)^2+(\lambda_2-\lambda_3)^2}}{\sqrt{(\lambda_1^2+\lambda_2^2+\lambda_3^2)}} \quad . \tag{9}$$

3 Results and Discussion

In order to choose an appropriate distribution $P(\Delta\bar{r})$ of random walking step lengths, we compare two situations with respectively Gaussian and uniform distributions, which are often used in simulations [10-12]. Then, the diffusion weighted images (DWI) of the myocytes are simulated and the influence of the water content ratio in different compartments upon diffusion anisotropy is analyzed by means of the diffusion tensor. Finally, the influence of membrane permeability upon diffusion anisotropy is also investigated.

3.1 Monte Carlo Simulation of the Restricted Diffusion

We assume that water molecules diffuse in two infinite parallel plates spaced by a distance of $2a$ (Eq.10). If the diffusion gradient is applied along the direction normal to the plates, the thus resulting diffusion corresponds to the restricted diffusion. However, if the gradient is added in the direction parallel to the plates, it then concerns free diffusion of the water molecules in this direction. For the restricted diffusion and the free diffusion, the corresponding analytical diffusion equations are given respectively by

$$E_{\mathrm{retrict}} = \sin^2(\pi qa)/(\pi qa)^2 \quad . \tag{10}$$

$$E_{\mathrm{free}} = \exp(-bD_0) \quad . \tag{11}$$

which correspond to two modeling situations.

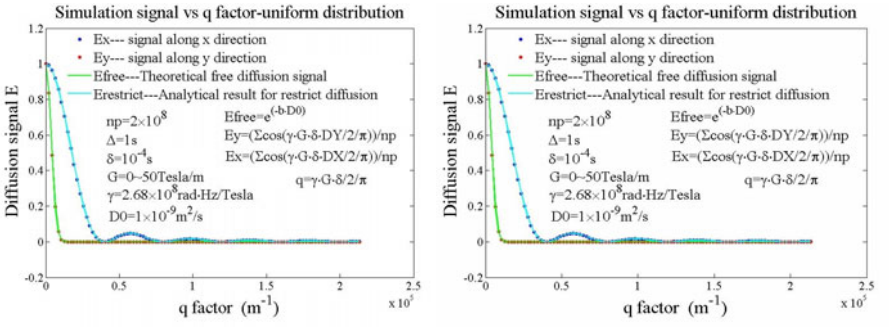

Fig. 1. Monte Carlo simulation of DMRI signal of diffusion between two plates

In all the simulations, the number of molecules was set to 2×10^8 in order to obtain the results with high accuracy. At the beginning, the molecules are uniformly distributed in space. Then, they walk randomly with either uniform or Gaussian distribution of walk step lengths, but with the same distribution of directions (between 0 and 2π). After a given time, according to equation (8), the diffusion signals in the directions both normal and parallel to the plate are calculated. All simulations were performed on a PC machine cluster; the computation time was about 16 hours. The simulation results with the corresponding parameters are illustrated in Fig. 1. It can be seen that the simulation with the uniform distribution conforms better to the theoretical results. For this reason, in the following, all the diffusion processes will be simulated using the uniform distributed walking step length.

3.2 Simulation of VCFS

In order to approximate the actual structure of myocytes, we represent it by a random hexagons combination. In the transverse plane, the myocyte location is randomly distributed on the surface. Based on the Voronoi theory, a myocyte is formed by combining the nearest neighbor hexagons. Fig.2 provides a histological image for the transverse section of myocytes and its corresponding simulation model. It can be seen that our model is fairly realistic, and that it can generate myocytes with certain regular organization but varying shapes.

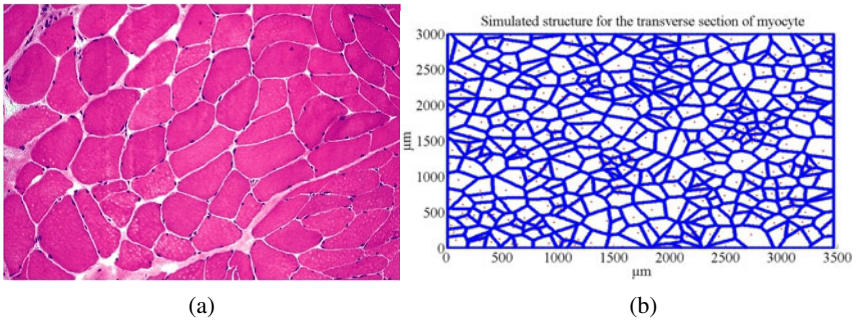

(a) (b)

Fig. 2. (a) histological image for the transverse section of myocyte (Reference [16]) (b) The VCFS transverse model

From this transverse slice, a three-dimensional myocyte is constructed by changing the length of the myocytes. By choosing the hexagon as the basic modeling element, we can control various parameters of diffusion simulation such as the boundary condition for the random walk, the simulation spatial resolution, the computation complexity, etc. In the present study, the hexagon edge length was chosen as 5μm.

3.3 DTI Simulation and Anisotropy Analysis

As mentioned in Section 2.2, diffusion tensor imaging data can be simulated by applying diffusion gradients along different directions. The DTI data are simulated at three different scales. The first DTI scale concerns that of one hexagon, which corresponds to one voxel having a dimension of 5x5x5 μm^3. The second scale is at the level of one myocyte whose spatial resolution is about 25μm, and the final scale is dealt with the simulation of several myoyctes. In the present study, we chose only four myocytes with a resolution of about 100μm, for the sake of the heavy computation load.

3.3.1 Influence of Water Content on Diffusion Anisotropy

From the research of Denis Le Bihan [17], it is considered that water molecules diffuse quickly in the intra and extra spaces, but diffuse slowly near and across the membrane. The dimension of the membrane of cardiac myocytes being about 7.5 nm [18], it is so small in comparison with that of cytoplasm and extracellular space that it will be ignored in the present simulation. The diffusion coefficient in the cytoplasm and the collagen is selected as the same, which is $D_0 = 1000\mu m^2/s$, because both of them belong to the quick diffusion region. Moreover, the dimension of water molecules is about 3.2Å, and in the cytoplasm the water content is 78%, of which 92% is immobilized [19]. Thus, for our voxel (8x8x8 μm^3), there are about 3×10^{11} water molecules. In practice, it is almost impossible to simulate with such a number of water molecules. A trade-off between computing time and simulation accuracy should then be done. We selected 1000 molecules for one voxel. For the diffusion gradient, the amplitude was chosen as 2 Tesla/μm (note however that, in real imaging, it is about 1.5 Tesla/m), the diffusion time as 50 ms, and the number of random walks during this period as 300. Since there are some contradictory conclusions in the literature about the water content in the myocyte and extracellular space, it is necessary to simulate the effects of the ratio of water contents on diffusion anisotropy. Fig. 3(a) shows a 3D simulated structure of myocytes, (b) a single transverse slice and (c) the corresponding diffusion image of the later in one gradient direction d (red color) which is illustrated in Fig.3(d). For this illustrated situation, water was distributed only in the extracellular space in order to distinguish it from the structure information.

To investigate the influence of water content in different compartments, the ratio of water content in cytoplasm and extracellular space was chosen respectively as 1/6, 1/5, 1/4, 1/3, 1/2, 1(Point1, Fig. 4(a)), 2, 3 (Point2, Fig. 4(a)), 4, 5 and 6. The simulation results are given in Fig. 4, where Fig. 4(a) shows the variation of diffusion anisotropy with the water content ratio changes in extracellular and intracellular spaces. We compare the diffusion images along the same direction for different water content ratio. It can be seen that for each pixel the diffusion signal intensity changes a

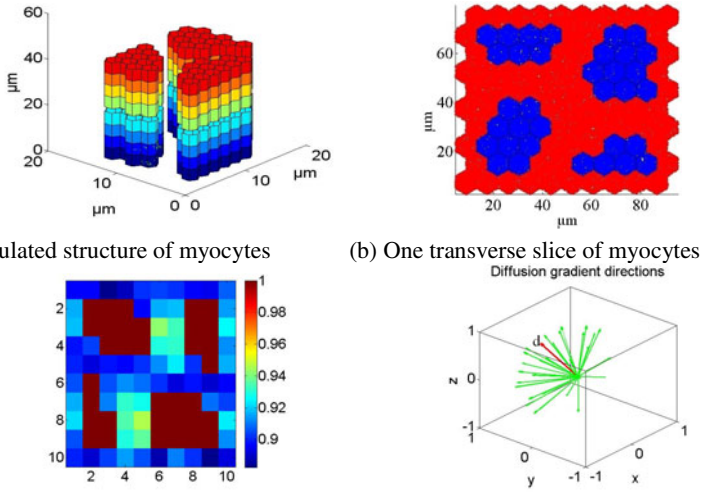

(a) 3D simulated structure of myocytes (b) One transverse slice of myocytes

(c) Simulated DWI for slice (b) indirection d (red) (d) Directions of diffusion gradient

Fig. 3. 3D Myocyte structure and diffusion image

little, which means, from a microscopic view, that the change in water content ratio does not influence greatly the anisotropy. This can also be verified by the diffusion tensor for each voxel shown in Fig. 4(b) and 4(c). However, for a larger scale of single myocyte or several myocytes, the diffusion FA increases if the water content in the myocyte is bigger than that in the extracellular medium, as illustrated by global diffusion tensor comparison in Fig. 4(b) and 4(c). This phenomenon is caused by the combination effects of diffusion in the intra- and extra- cellular compartments in the large scale measurement. All these imply that for modeling MRI diffusion signal with DTI in large scales, the water content influence should be taken into account.

3.3.2 Influence of Permeability on Diffusion Anisotropy

According to [20], there are some aqueous pores in the myocyte membrane, which allow water molecules to exchange between different compartments (intra- and extra-cellular). Following [21], the membrane permeability of a myocyte ranges from 0 to 100 μm/s. During their random walk process, water molecules will pass through the membrane with a certain probability p, determined by the permeability p_t, the diffusion coefficient D_0 and the random walk step length s. Their relationships is ruled by

$$p = p_t \times s / D_0 \quad . \tag{12}$$

The simulation results are shown in Fig. 5.

The results show that the diffusion anisotropy decreases with the increase of the membrane permeability. In the present work, walk step length is 1μm that corresponds to a diffusion time of 1/6 ms for one step. In this condition, when the membrane permeability is smaller than 50μm/s, its influence can be ignored.

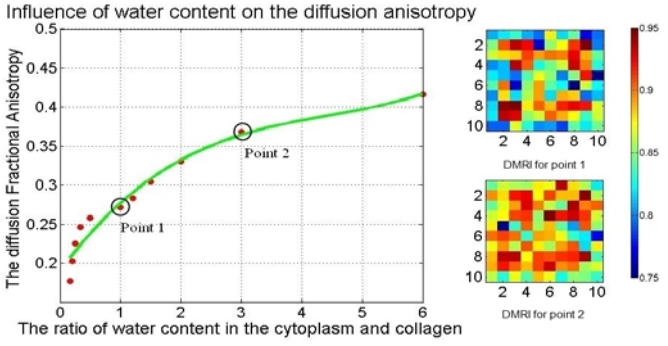

(a) Influence of water content on the FA and DWI of the myocyte slice (Fig.4(b)) in the same gradient direction d for two different water content ratios 1 (Point 1) and 3 (Point 2)

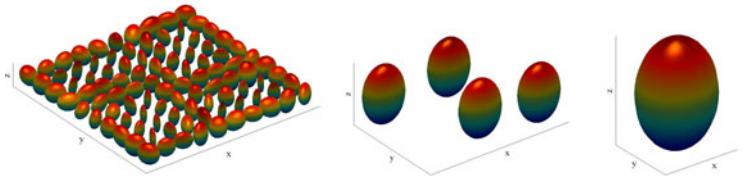

(b) 3D Diffusion Tensor of one hexagon, one myocyte and four myocytes for Point 1

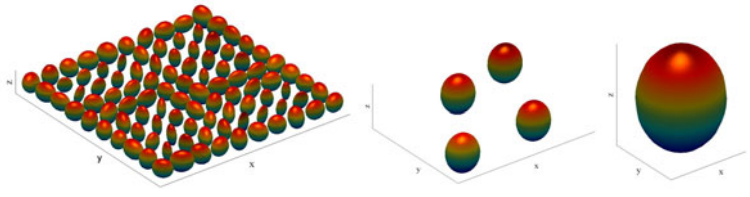

(c) 3D Diffusion Tensor of one hexagon, one myocyte and four myocytes for Point 2

Fig. 4. Influence of water content on the diffusion FA

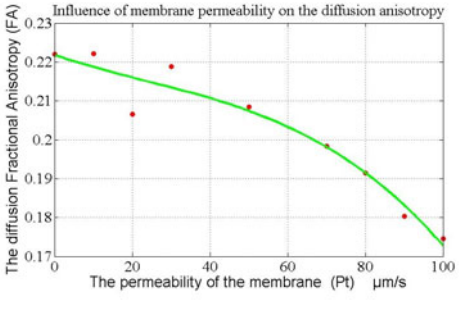

Fig. 5. Influence of membrane permeability on the FA

In practice, diffusion time in DMRI ranges from several ms to several seconds. As a result, for such long diffusion process, the contribution of permeability to FA should be considered accordingly.

4 Conclusion

A fairly realistic virtual cardiac fiber structures (VCFS) model has been constructed, and its diffusion weighted image and diffusion tensor image were simulated by Monte Carlo method. From the thus simulated images, the influences of the water content and membrane permeability upon diffusion anisotropy have been investigated. The results show that the diffusion anisotropy increases with the increase of ratio of water content between intra- and extra- cellular media, and that it decreases with the increase of membrane permeability. Consequently, for different spatial resolutions in practical imaging, the contribution to FA of water content in different compartments and permeability should be taken into account accordingly. For the future work, we will improve the VCFS model to make it more realistic and compare the thus obtained results with practical imaging techniques such as polarized optical imaging.

Acknowledgements

This work was supported by the National Natural Science Foundation of China (60777004), International S&T Cooperation Project of China (2007DFB30320), and French ANR 2009 (under ANR-09-BLAN-0372-01).

References

1. Le Bihan, D.: Looking into the functional architecture of the brain with diffusion MRI. International Congress Series. Elsevier, Amsterdam (2006)
2. Kingsley, P.B.: Introduction to diffusion tensor imaging mathematics: Part I. Tensors, rotations, and eigenvectors. Concepts in Magnetic Resonance Part A 28, 101–122 (2006)
3. Descoteaux, M., Angelino, E., Fitzgibbons, S., Deriche, R.: Apparent diffusion coefficients from high angular resolution diffusion imaging: Estimation and applications. Magnet. Reson. Med. 56, 395–410 (2006)
4. Özarslan, E., Koay, C.G., Basser, P.J.: Remarks on q-space MR propagator in partially restricted, axially-symmetric, and isotropic environments. Magnetic Resonance Imaging 27, 834–844 (2009)
5. Tuch, D.S.: Q-ball imaging. Magnet. Reson. Med. 52, 1358–1372 (2004)
6. Le Bihan, D., Poupon, C., Amadon, A., Lethimonnier, F.: Artifacts and pitfalls in diffusion MRI. Journal of Magnetic Resonance Imaging 24, 478–488 (2006)
7. Assaf, Y., Freidlin, R.Z., Rohde, G.K., Basser, P.J.: New modeling and experimental framework to characterize hindered and restricted water diffusion in brain white matter. Magnetic Resonance in Medicine 52, 965–978 (2004)
8. Severs, N.J.: The cardiac muscle cell. Bioessays 22, 188–199 (2000)
9. Duh, A., Mohori, A., Stepinik, J.: Computer simulation of the spin-echo spatial distribution in the case of restricted self-diffusion. Journal of Magnetic Resonance 148, 257–266 (2001)
10. Cai, C., Chen, Z., Cai, S., Zhong, J.: Propagator formalism and computer simulation of restricted diffusion behaviors of inter-molecular multiple-quantum coherences. Physica B: Condensed Matter 366, 127–137 (2005)

11. Fieremans, E., De Deene, Y., Delputte, S., Özdemir, M.S., D'Asseler, Y., Vlassenbroeck, J., et al.: Simulation and experimental verification of the diffusion in an anisotropic fiber phantom. Journal of Magnetic Resonance 190, 189–199 (2008)
12. Avram, L., Özarslan, E., Assaf, Y., Bar-Shir, A., Cohen, Y., Basser, P.J.: Three-dimensional water diffusion in impermeable cylindrical tubes: theory versus experiments. NMR in Biomedicine 2, 888–898 (2008)
13. Heidi, J.B., Timothy, E.J.B.: Diffusion MRI, 1st edn., p. 8. Elsevier, Amsterdam (2009)
14. Kingsley, P.B.: Introduction to diffusion tensor imaging mathematics: Part II. Anisotropy, diffusion-weighting factors, and gradient encoding schemes. Concepts in Magnetic Resonance Part A 28, 123–154 (2006)
15. Kingsley, P.B.: Introduction to diffusion tensor imaging mathematics: Part III. Tensor calculation, noise, simulations, and optimization. Concepts in Magnetic Resonance Part A 28, 155–179 (2006)
16. Skeletal, M., Reid, R.H.J., Lucia, L.B.: Histology for Pathologists, 3rd edn., p. 201. Williams & Wilkins, Baltimore (2009)
17. Bihan, D.L.: The 'wet mind': water and functional neuroimaging. Physics in medicine and biology 52, R57–R90 (2007)
18. Iaizzo, P.A.: Handbook of Cardiac Anatomy, Physiology, and Devices, 2nd edn. (2009)
19. Friedrich, M.G.: Myocardial edema—a new clinical entity? Nature Reviews Cardiology (2010)
20. Egan, J.R., Butler, T.L., Au, C.G., Tan, Y.M., North, K.N., Winlaw, D.S.: Myocardial water handling and the role of aquaporins. Biochimica et Biophysica Acta (BBA)-Biomembranes 1758, 1043–1152 (2006)
21. Ogura, T., Imanishi, S., Shibamoto, T.: Osmometric and water-transporting properties of guinea pig cardiac myocytes. The Japanese Journal of Physiology 52, 333–342 (2002)